WEP Warwick Evans Publishing

International Journal of Materials Science and Technology Studies

ISSN: 3006-7693 (Print), ISSN: 3006-3744 (Online) | Volume 3, Number 1, Year 2025
DOI: https://doi.org/10.62051/ijmsts.v3n1.02
Journal homepage: https://wepub.org/index.php/IJMSTS/index

Study on the Performance of Different Modification Conditions on the Activity of Red Mud

Aonan Zhao, Shiying Chen

School of Resources and Environment, Henan Polytechnic University, Jiaozuo 454003, China

ABSTRACT

Red mud is an industrial solid waste produced during alumina extraction from bauxite. This study aims to enhance red mud's reactivity and develop a composite cementitious material to increase its utilization rate. The methods used include individual red mud calcination and co-calcination with calcium carbide slag (RM-CS). The physical and chemical properties of red mud were assessed using X-ray diffraction (XRD) and thermogravimetric-differential scanning calorimetry (TG-DSC) analyses. Results show that dolomite ($CaMg(CO_3)_2$) in red mud starts to decompose at 500°C and is nearly fully decomposed by 900°C. The physical and chemical properties of the composite cementitious material were analyzed via XRD and compressive strength tests. The findings indicate that the 28-day compressive strength of the red mud composite material reaches 60 MPa, while the RM-CS composite material reaches 64 MPa. Toxicity leaching results indicate that the heavy metal ion content in the composite material complies with standard requirements, suggesting that the composite cementitious material is environmentally friendly.

KEYWORDS

Red mud; Calcium carbide slag; High-temperature calcination; Co-calcination

1. INTRODUCTION

Red mud is an industrial solid waste produced during alumina refining from bauxite. Named for its high iron oxide content and reddish soil-like appearance, it is called red mud [1]. As the world's leading alumina producer, China accounts for 55% of global alumina output, discharging 1.5–2.5 tons of red mud per ton of alumina produced [2]. In 2023, China's alumina production reached 82.441 million tons, with over 107 million tons of red mud discharged, but the red mud utilization rate was only 9.8% [3]. The strong alkalinity, complex chemical composition, and heavy metal ion leaching characteristics of red mud have impeded its widespread application [4]. Currently, the primary method for handling red mud is open-air storage, which not only occupies substantial land resources but also causes severe pollution as the contained heavy metals leach into soil and groundwater with rainwater [5]. To date, China has made significant efforts in red mud management and utilization, yet there remains a need to develop an economical and sustainable utilization method [2].

In traditional building material production, the consumption of natural resources like limestone is substantial. With the growing emphasis on circular economy and sustainable development, there is an increasing search for and utilization of industrial by-products as alternative raw materials [6]. Calcium carbide slag, an industrial by-product from the acetylene production process via calcium carbide hydrolysis, contains over 80% $Ca(OH)_2$, making it an ideal limestone substitute. Using calcium carbide slag not only reduces natural limestone use but also, due to its excellent thermal decomposition properties, provides a strong basis for replacing limestone in building material sintering.

In recent years, co-calcination of red mud with other solid wastes has emerged as a research hotspot. Co-calcination not only effectively reduces red mud's alkalinity but also leverages calcium carbide slag's active components to activate and solidify valuable metal oxides in red mud, producing new materials with potential applications [7-8]. Scholars have researched the co-calcination of red mud with industrial solid wastes like fly ash, coal gangue, and blast furnace slag, improving material mechanical properties and durability. Guo Changlu prepared high-iron aluminates cementitious materials from red mud, steel slag, and other solid wastes for concrete use, meeting both mechanical and permeability specifications [9]. Dong found that pre-treated red mud mixed with phosphogypsum as supplementary cementitious materials effectively improves cement system density [10]. Ding Xiang et al. [11] prepared red mud-high alumina fly ash-based porous ceramics via high-temperature melting and foaming. Lu Fanghai et al. [12] achieved calcium recycling and simultaneous aluminum and sodium recovery through red mud and phosphogypsum co-treatment. Liang Xu et al. [13] found that adding red mud to cement improves early cement-stabilized broken stone strength, with cement hydration products continuing to react with red mud. Zhou Libo et al. [14] studied the synergistic cementing effects of composite mortars from binary solid wastes. Ou Xiaoduo [15] found that red mud-metakaolin addition to cement mortar improves composite cement mortar mechanical properties.

Based on the aforementioned, this study primarily investigated the high-temperature calcination treatment of red mud and red mud-calcium carbide slag samples. The aim was to modify the chemical composition of red mud via high temperatures to enhance its reactivity, and to investigate the hydration mechanisms and leaching behavior of composite cementitious materials under various calcination temperatures. This research conducted a detailed examination of the hydration products of the composite materials to elucidate their hydration mechanisms, and performed leaching toxicity tests to assess the environmental safety of the composite materials.

2. EXPERIMENTAL

2.1. Experimental Raw Materials

The red mud used in the experiment was sourced from Hebei, the calcium carbide slag from Henan Energy and Chemical Group Hebi Coal Chemical Co., Ltd., and the P·O 42.5 grade cement from Jiaozuo Qianye Cement Factory. X-ray fluorescence (XRF) was used to analyze the chemical compositions of the red mud and calcium carbide slag, with results shown in Table 1. The main components of red mud are Fe_2O_3, SiO_2, Al_2O_3, CaO, and Na_2O, comprising over 87% of the total mass. The primary constituent of calcium carbide slag is CaO, constituting over 90% of the total mass.

Table 1. Main Chemical Composition of Raw Materials (Mass Fraction)

Chemical composition	SiO_2	Al_2O_3	Fe_2O_3	CaO	NaO_2	MgO	TiO_2	SO_3	other
Red mud	19.80	20.60	33.24	7.32	7.12	5.62	4.23	0.66	1.41
Calcium Carbide Slag	3.71	1.58	0.24	90.34	—	0.28	—	2.54	1.31

X-ray diffraction (XRD) was used to determine the mineral compositions of red mud and calcium carbide slag, with results shown in Figure 1. The main mineral components of red mud are dolomite ($CaMg(CO_3)_2$), hematite (Fe_2O_3), talc ($Mg_3Si_4O_{10}(OH)_2$), and quartz (SiO_2). The primary mineral constituents of calcium carbide slag are portlandite ($Ca(OH)_2$) and calcite ($CaCO_3$). The particle size distribution of red mud and calcium carbide slag was measured using a Malvern Mastersizer 2000 laser particle size analyzer, with results shown in Figure 2. The specific surface area of red mud is 2975 m²/kg, with a median particle size of 10.7 μm, indicating relatively fine particles. The specific surface area of calcium carbide slag is 582.8 m²/kg, with a median particle size of 37 μm. Figure 3 shows the microscopic morphologies of red mud and calcium carbide slag.

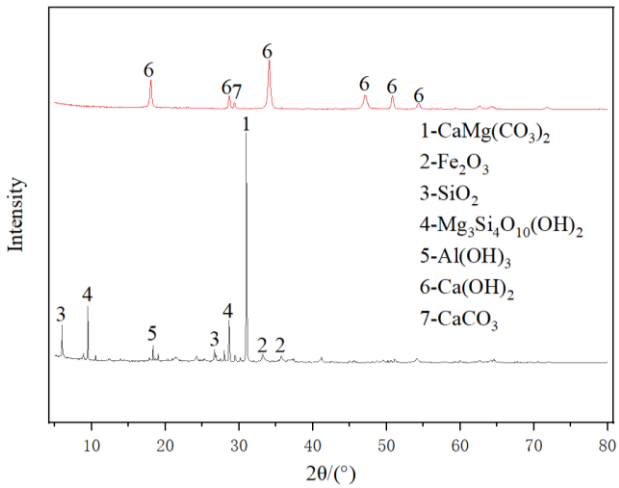

Figure 1. XRD patterns of Red Mud (RM) and Calcium Carbide Slag (CS)

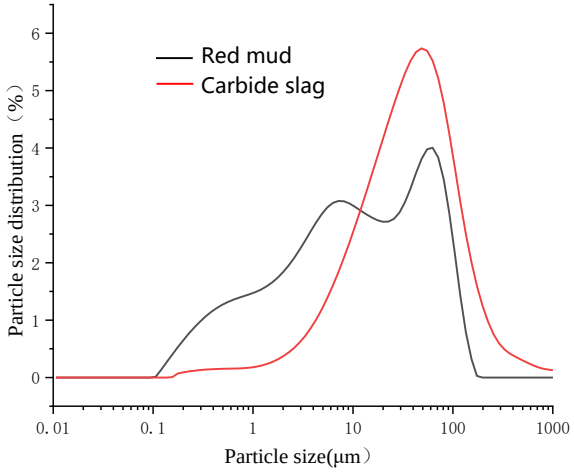

Figure 2. Particle Size Distribution of Red Mud (RM) and Calcium Carbide Slag (CS)

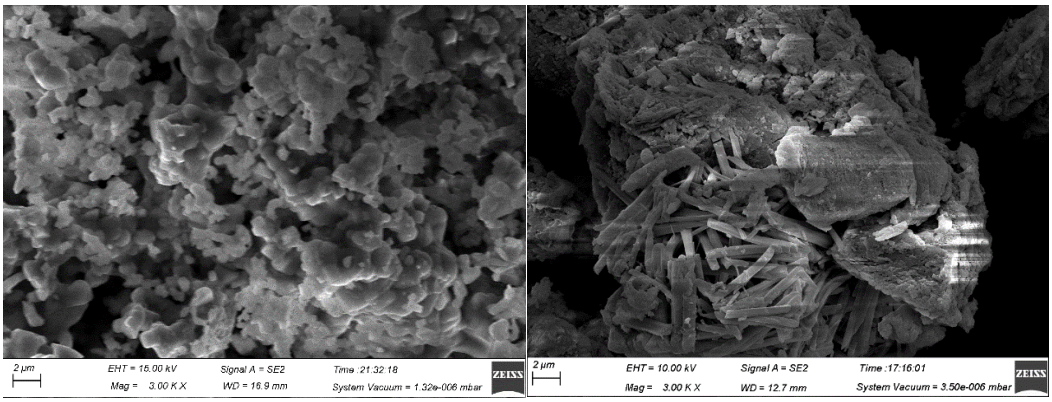

Figure 3. SEM Images of Red Mud (RM) (left) and Calcium Carbide Slag (CS) (right)

2.2. Pre-treatment of Experimental Raw Materials

The red mud raw material was ground, passed through a 60-mesh sieve, and placed in an alumina crucible for calcination in a resistance furnace. Calcination temperatures were set at 800°C, 900°C, 1000°C, and 1100°C, with a heating rate of 10°C/min. After reaching the set temperature, the material was held for 2 hours, then cooled to room temperature. The calcined clinker was ground and passed

through a 60-mesh sieve to obtain the modified red mud. For reference, the calcined red mud is denoted as RM_t (where t = 800°C, 900°C, 1000°C, 1100°C). For example, RM800°C refers to red mud calcined at 800°C. Red mud and calcium carbide slag were mixed evenly at a ratio of 20:4.2 and placed in a resistance furnace for calcination. Calcination temperatures were set at 900°C, 1000°C, and 1100°C, with the same heating rate and holding time as mentioned above, then cooled to room temperature, and denoted as RM-CS_t (where t = 900°C, 1000°C, 1100°C).

2.3. Experimental Design

Given the low reactivity of the original red mud, it must be calcined and modified for secondary utilization. Based on this, the study focuses on the reactivity changes of red mud and red mud co-calcined with calcium carbide slag. The compressive strength of the composite material at 3, 7, and 28 days serves as the evaluation criteria to observe reactivity changes in the samples after calcination under different conditions.

2.4. Specimen Preparation and Testing

2.4.1. Specimen Preparation

To understand the hydration mechanism and study the microstructure and crystal phases of the hydration products, calcined samples were mixed with cement at a 15:85 ratio to prepare specimens. The water-to-binder ratio was set at 0.4. Following GB/T 17671-1999 "Method of Testing Compressive and Flexural Strength of Cement Mortar (ISO Method)", the composite material paste was thoroughly mixed and poured into 40mm×40mm×160mm molds. After 24 hours of curing at room temperature, the specimens were demolded. The demolded specimens were cured in a chamber at 28±1℃ and over 95% humidity until reaching 3, 7, and 28 days.

2.4.2. Analysis Methods

Samples were dried at 105°C for 12 hours and ground into powder (≤75μm) for chemical composition analysis using X-ray fluorescence spectroscopy (XRF, Bruker Tiger S8). One gram of the raw material was dissolved in 10.0 g of deionized water to prepare a solution, and its pH was measured using an automatic titrator. The phase composition of the samples and calcined samples was analyzed using an X-ray diffractometer (XRD, Rigaku Ultima IV X). The center part of the specimen was immersed in anhydrous ethanol for 24 hours to terminate hydration, then dried in an oven at 60°C until a constant weight was reached, and ground through a 75 μm square mesh sieve for XRD detection. XRD testing conditions: Cu target, 40 kV and 40 mA, scanning range 5° to 80°, scanning rate 10°/min.

A Merlin Compact field-emission scanning electron microscope (FESEM) was used to analyze the microstructure morphology. Due to the samples' poor conductivity, a PECSII685.C sputtering coater was used to apply a gold coating to the dried samples for 180 seconds. The device is equipped with an OXFORD EDS (energy-dispersive X-ray spectroscopy) system to test the chemical composition of selected areas within the samples at 15 kV. Thermogravimetric-differential scanning calorimetry (TG-DSC) was used to detect mass changes in red mud as the temperature increased from 25°C to 1000°C at a rate of 20°C/min.

In accordance with HJ 557−2010 "Solid Waste - Extraction Procedure for Leaching Toxicity - Horizontal Vibration Method", the original red mud and broken 28-day-old specimens were collected, ground through a 3 mm square mesh sieve, and 20 g of the sample was poured into a 500 ml conical flask. Deionized water was added at a solid-to-liquid ratio of 1:10, the flask was tightly capped, and placed in a horizontal shaker for 8 hours of oscillation. After standing for 16 hours, the supernatant was collected. The concentration of heavy metal ions (As, Cr, V, Zn, Mn) in the composite material was detected using a Perkin Elmer Optima 8000 ICP-OES (inductively coupled plasma optical emission spectrometer).

3. RESULTS AND DISCUSSION

3.1. Compressive Strength of Red Mud Composite Materials

Figure 4 shows the compressive strength of composite materials prepared from red mud and red mud-calcium carbide slag at different ages. The compressive strengths of the blank control group (pure cement specimens) were 46.6 MPa at 3 days, 50.4 MPa at 7 days, and 62 MPa at 28 days. As Figure 4 shows, the compressive strength of the original red mud was the lowest, indicating it lacks pozzolanic activity when uncalcined and can only serve as a filler. The compressive strength reached its maximum when the red mud was calcined at 900°C, with values of 46.6 MPa at 3 days, 50.1 MPa at 7 days, and 60 MPa at 28 days. However, the strength of specimens prepared from individually calcined red mud was lower than that of the pure cement control group, suggesting that both the original and calcined red mud are unsuitable for use as cement clinker. Nevertheless, Figure 4 shows that the unconfined compressive strength of the composite material significantly increased after the red mud was mixed with calcium carbide slag and calcined. Compared to specimens incorporating individually calcined red mud, the compressive strengths of the RM-CS composite material at three different ages were all improved, and the composite material incorporating RM-CS1000°C achieved the control group's compressive strength at 28 days. This may be due to the increased free alkali after calcination with calcium carbide slag, increasing the number of silicate and aluminate tetrahedra monomers and alkalinity during activation. High alkalinity not only aids in the dissolution of aluminosilicate minerals but also promotes the hydration reaction, forming more amorphous gel phases and thus providing higher strength. As Table 1 shows, calcium carbide slag contains significant CaO, and dissolved Ca^{2+} reacts with silicates and aluminates to form more hydration products (such as calcium silicate hydrate and calcium aluminate hydrate), increasing the strength of the prepared composite material. However, when the calcination temperature is too high, the situation changes. Excessively high temperatures may cause the decomposition or volatilization of certain mineral components, disrupting the specimen's structural integrity. Additionally, excessively high temperatures may trigger adverse chemical reactions, such as excessive sintering or melting, leading to defects or cracks within the specimen, significantly reducing its strength. On the other hand, when the temperature is too high, the reaction rate may be too fast, causing rapid reactions between red mud and calcium carbide slag components or the formation of unstable intermediate products, disrupting the specimen's internal structural balance and reducing the cementitious material's strength.

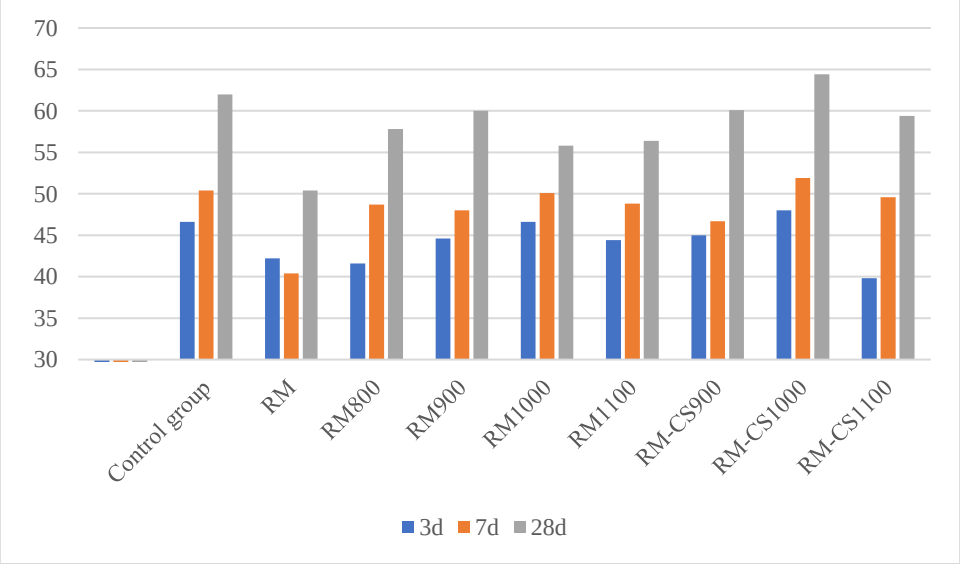

Figure 4. Compressive Strength of Red Mud Composite Materials Calcined at Different Temperatures

3.2. Thermogravimetric Analysis

The TG-DSC curve of red mud is shown in Figure 5. As the temperature rises from room temperature to 1000°C, the total mass loss of red mud is 14.3%, divided into three stages: room temperature to 250°C, 250°C to 600°C, and 600°C to 1000°C. In the first stage, mass loss is primarily due to the evaporation of physical water and the decomposition of crystalline water in the original red mud. In the second stage, two endothermic peaks appear. The endothermic peak at 267°C corresponds to the dehydroxylation decomposition of gibbsite ($Al(OH)_3$) to form boehmite and χ-Al_2O_3, while the endothermic peak at 460°C corresponds to the first-stage decomposition of $CaMg(CO_3)_2$. $CaMg(CO_3)_2$, a composite compound of $MgCO_3$ and $CaCO_3$, decomposes in two steps during heating, as shown in Equations (1) and (2). The lower decomposition temperature of $MgCO_3$ compared to pure $MgCO_3$ is due to its combination with $CaCO_3$, reducing $MgCO_3$'s activity. The mass loss in the third stage is mainly due to the decomposition of $CaCO_3$ in $CaMg(CO_3)_2$ and $Mg_3Si_4O_{10}(OH)_2$.

$$CaMg(CO_3)_2 \rightarrow CaCO_3 \cdot (1-x)\ MgCO_3 + xMgO + xCO_2 \quad (1)$$

$$CaCO3 \rightarrow (1-y)CaCO_3 + yCaO \quad (2)$$

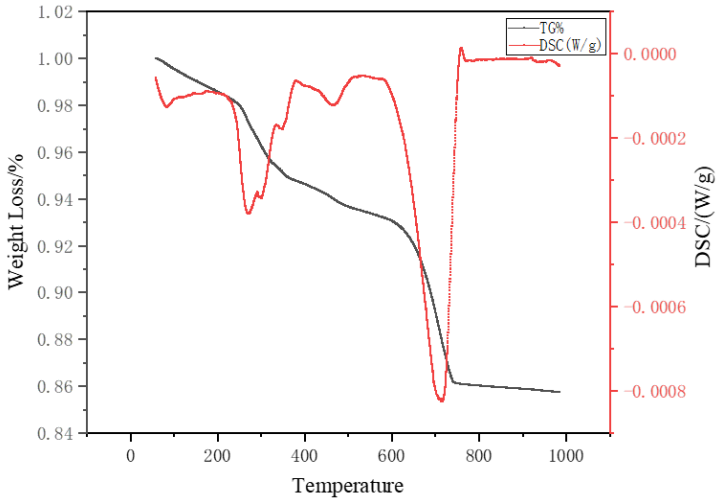

Figure 5. Thermogravimetric (TG-DSC) Curves of Red Mud

3.3. Phase Composition of Red Mud Composite Materials

XRD analysis was conducted on RM, RM800°C, RM900°C, RM1000°C, RM1100°C, RM-CS900°C, RM-CS1000°C, and RM-CS1100°C. As Figure 6 shows, after high-temperature calcination at 800°C, the XRD patterns did not detect the diffraction peaks of gibbsite ($Al(OH)_3$) and dolomite ($CaMg(CO_3)_2$), indicating they had completely decomposed before 800°C, consistent with the thermogravimetric test results. When the temperature was raised to 900°C, the diffraction peak of $CaAl_2Si_2O_8$ appeared. Concurrently, the diffraction peak of SiO_2 decreased. As the temperature continued to rise, numerous diffraction peaks of $NaAlSiO_4$ emerged, which also explains the increased strength of the specimens compared to those prepared from the original samples. Regardless of the temperature increase, the mineral phase of Fe_2O_3 remained unchanged.

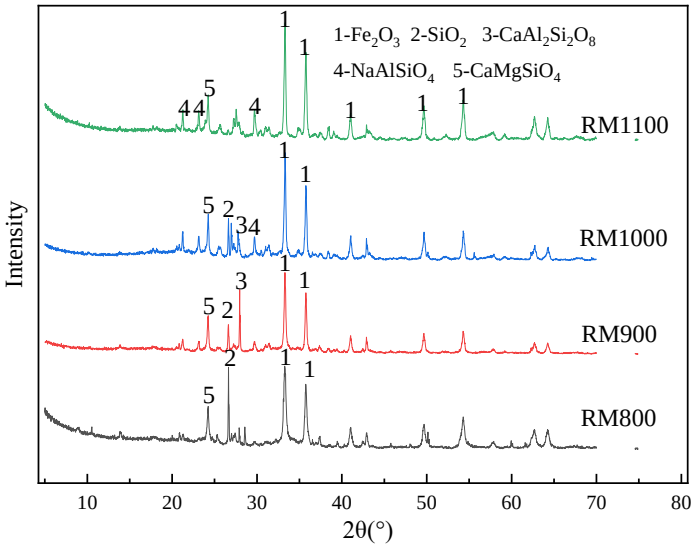

Figure 6. XRD spectra of RM800°C, RM900°C, RM1000°C, and RM1100°C

Figure 7 shows the XRD spectra of RM-CS900°C, RM-CS1000°C, and RM-CS1100°C. As can be seen from the figure, when the calcination temperature is 900°C, the diffraction peaks of SiO_2 and $CaCO_3$ appear, when the calcination temperature is 1000°C, the diffraction peaks of $MgSiO_3$ and $AlSiO_5$ appear, and when the calcination temperature is 1100°C, the diffraction peaks of $NaAlSiO_4$ and $CaAl_2SiO_7$ appear.

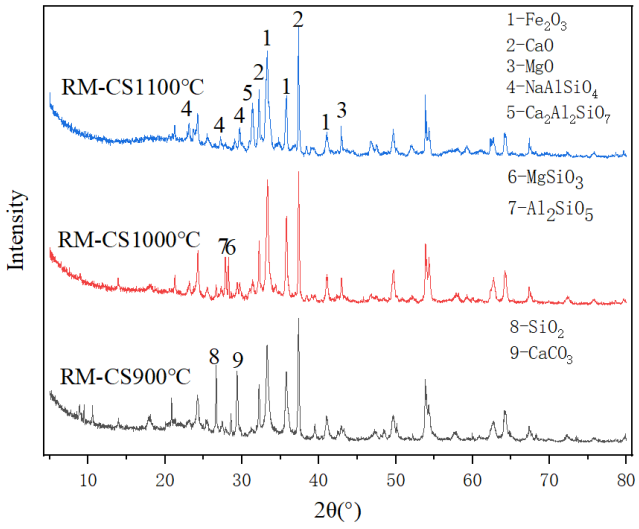

Figure 7. XRD spectra of RM-CS900°C, RM-CS1000°C, and RM-CS1100°C

Figure 8 shows the XRD patterns of the pure cement control group, RM, RM900°C, and RM-CS1000°C specimens after 28 days of hydration, followed by immersion in anhydrous ethanol to terminate hydration. As Figure 8 shows, the hydration products of the four groups of specimens after 28 days of hydration are essentially similar, with the main hydration product minerals being $Ca(OH)_2$, C_2S, and C_3S. The diffraction peaks of unhydrated $CaMg(CO_3)_2$ were detected in RM and RM900°C, which may also contribute to the low strength of the composite materials. The active SiO_2 and Al_2O_3 in red mud gradually consume the alkaline hydration products in the reaction system during hydration, reducing the $Ca(OH)_2$ crystal diffraction peaks in the diffraction patterns of RM and RM900°C. The active SiO_2 and Al_2O_3 in red mud and the $Ca(OH)_2$ in calcium carbide slag undergo partial reactions, so the diffraction peak of $Ca(OH)_2$ in calcium carbide slag is only slightly reduced. It can overlap with C-S-H gel, ettringite, and other hydration products to form a dense microstructure, thereby increasing the strength of the specimens.

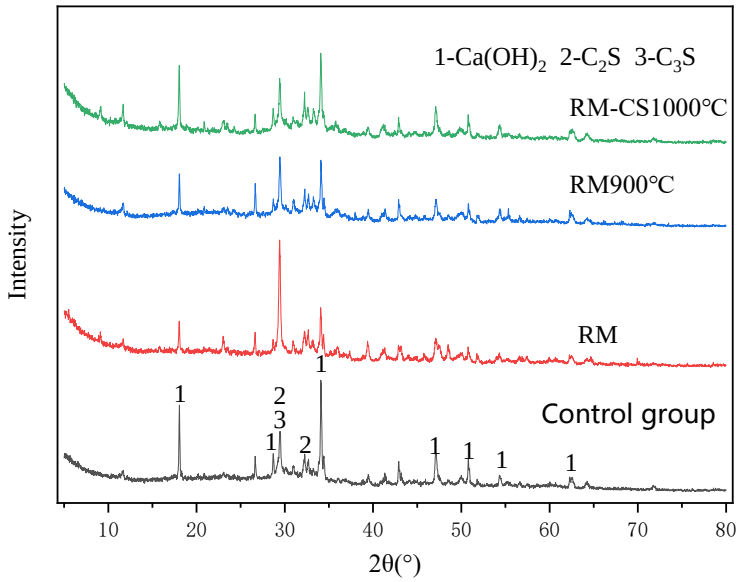

Figure 8. XRD Patterns of Pure Cement Control, RM, RM900°C, and RM-CS1000°C

3.4. Microstructure of Red Mud Composite Materials

Cementitious samples obtained through different thermal activation methods exhibit unique microstructural characteristics at various curing periods. Since the RM900°C directly activated red mud-based cementitious material and the RM-CS1000°C activated red mud-based cementitious material demonstrated better mechanical properties at 28 days, these two thermal activation pre-treatment methods can promote the hydration reaction of the cementitious samples. Therefore, samples A and B were chosen to study the microstructure of the cementitious materials, and further investigation was conducted on the hydration reaction mechanism of the cementitious samples prepared from pre-activated red mud under different conditions. As can be seen from Figure 9, the strength of the sample prepared after calcination is high and the strength of the sample prepared is increased compared to that prepared as it is.

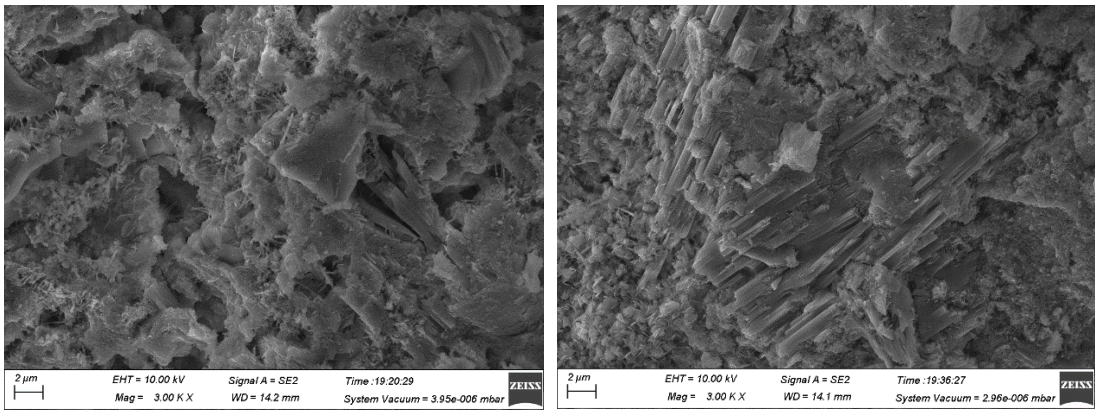

Figure 9. Microscopic morphology of the test blocks prepared at RM900°C (left) and RM-CS1000°C (right)

3.5. Heavy Metal Leaching Test

This study measured the heavy metal ion concentrations in red mud, 28-day red mud composite materials, and 28-day red mud-calcium carbide slag composite materials. The leaching results are shown in Table 2. The leaching toxicity results in Table * were compared with national standards to ensure that the materials' use does not exceed limit values posing a threat to public health. The results

indicate that the leaching concentrations of As, Cr, V, Zr, and Mn in all composite material samples are significantly lower than the standard limits.

Table 2. Leaching table of heavy metal ion concentration

Samples	As	Cr	V	Zr	Mn
GB5749-2022	0.01	0.05	0.01	—	—
RM	0.033	0.036	0.047	—	—
28d RM	—	—	—	—	—
28d RM800℃	—	0.029	—	—	—
28d RM900℃	—	0.036	—	—	—
28d RM1000℃	—	0.031	—	—	—
28d RM1100℃	—	0.007	—	—	—
28d RM-CS900℃	—	0.032	—	—	—
28d RM-CS1000℃	—	0.033	—	—	—
28d RM-CS1100℃	—	0.005	—	—	—

4. CONCLUSIONS

This study used red mud and calcium carbide slag as raw materials, enhancing red mud's reactivity through individual calcination and co-calcination with calcium carbide slag. The calcined clinker was then used to prepare composite materials, with the compressive strength of the specimens serving as the evaluation criterion. The study investigated the effects of different calcination conditions on red mud's reactivity enhancement. The main conclusions are: Calcination can cause intense thermal motion of particles in red mud at high temperatures, leading to the decomposition of certain minerals and thereby enhancing its reactivity. The optimal calcination temperature for individual red mud was determined to be 900°C, where the calcination activation effect was the best, increasing the 28-day compressive strength of the composite material from 50.4 MPa to 60 MPa. However, based on the overall compressive strength results, the highest reactivity enhancement of red mud was achieved through co-calcination with calcium carbide slag at 1000°C, increasing the 28-day compressive strength of the composite material from 50.4 MPa to 64.4 MPa, surpassing the pure cement control group at 28 days.

REFERENCES

[1] Wang S, Jin H, Deng Y, et al. Comprehensive utilization status of red mud in China: A critical review [J]. Journal of Cleaner Production, 2021, 289: 125136.

[2] Liu Xiaoming, Zhang Zengqi, Li Yu, et al. Research progress on the utilization of red mud in building materials and composite polymer materials [J].Materials Reports, 2023, 37(10):15-28.)

[3] Niu A, Lin C. Trends in research on characterization, treatment and valorization of hazardous red mud: A systematic review [J]. Journal of Environmental Management, 2024, 351: 119660.

[4] Soni A, Das P K, Hashmi A W, et al. Challenges and opportunities of utilizing municipal solid waste as alternative building materials for sustainable development goals: A review [J]. Sustainable Chemistry and Pharmacy, 2022, 27: 100706.

[5] Zhao Liwen, Zhu Ganyu, Li Shaopeng, et al. Research progress on characteristics and comprehensive utilization of calcium carbide slag [J].Clean Coal Technology, 2021, 27(03):13-26.)

[6] Wang S, Pan H, Xiao C, et al. Preparation and mix proportion optimization of red mud-fly ash-based cementitious material synergistic activated by carbide slag and MSWIFA [J]. Construction and Building Materials, 2024, 415: 135032.

[7] Shi Y, Zhao Q, Xue C, et al. Preparation and curing method of red mud-calcium carbide slag synergistically activated fly ash-ground granulated blast furnace slag based eco-friendly geopolymer [J]. Cement and Concrete Composites, 2023, 139: 104999.

[8] Guo Changlu, Gao Yifan, Li Zhaofeng. Preparation of ferroaluminate phase cementitious materials from metallurgical waste residue [J]. Journal of Materials and Metallurgy, 2020, 19 (02): 105-112. DOI:10.14186/j.cnki.1671-6620.2020.02.004.

[9] Shuangkuai D, Qi Z, Liangliang C, et al. Reuse of Pretreated Red Mud and Phosphogypsum as Supplementary Cementitious Material [J]. Sustainability, 2023, 15 (4):2856-2856.

[10] Ding Xiang, Pan Kaikai, Peng Bo, et al. Preparation of red mud-high alumina fly ash-based porous ceramics by melt foaming method [J]. Journal of the Chinese Ceramic Society, 2022, 50(3):713-722.

[11] Lu Fanghai, Chai Hongyun, He Haijun et al. Gypsum-red mud co-treatment resource utilization: small-scale and pilot-scale tests [J/OL]. Environmental Engineering, 1-10 [2024-03-16].

[12] Liang Xu, Liang Naixing, Zeng Jianmin, et al. JOURNAL OF CHONGQING JIAOTONG UNIVERSITY (NATURAL SCIENCE EDITION), 2008, 27(6): 1086-9.

[13] Zhou Libo, Chen Ping, Hu Cheng, et al. Hydration hardening characteristics of steel slag-red mud-cement-based composite mortar [J]. Bulletin of the Chinese Ceramic Society, 2023, 42(08):2837-2845.

[14] Ou Xiaoduo, Zeng Yuchu, Jiang Jie, et al. Effect of red mud-metakaolin compound on mechanical properties and hydration characteristics of cement mortar [J]. Chinese Journal of Materials Science and Engineering, 2023, 41(05):753-759.

[15] Ministry of Environmental Protection of the People's Republic of China. Solid waste leaching toxicity leaching method: HJ 557−2010 [S]. Beijing: Standards Press of China, 2010. HJ 557−2010 [S]. Beijing: China Standard Press, 2010.